Clim. Past Discuss., https://doi.org/10.5194/cp-2018-2
Manuscript under review for journal Clim. Past
Discussion started: 21 February 2018

The effect of high dust amount on the surface temperature during the Last Glacial Maximum: A modelling study using MIROC-ESM

Rumi Ohgaito[1], Ayako Abe-Ouchi[2,1], Ryouta O'ishi[2], Toshihiko Takemura[3], Akinori Ito[1], Tomohiro Hajima[1], Shingo Watanabe[1], Michio Kawamiya[1]

[1]Japan Agency for Marine-Earth Science and Technology, Yokohama, 236-0001, Japan
[2]Atmosphere Ocean Research Institute, University of Tokyo, Kashiwa, Chiba 277-8564, Japan
[3]Research Institute for Applied Mechanics, Kyushu University, Fukuoka, 816-8580 Japan

Correspondence to: Rumi Ohgaito (ohgaito@jamstec.go.jp)

Abstract. The effect of aerosols is one of the many uncertain factors in projections of the future climate. However, the behaviour of mineral dust aerosol (dust) can be investigated in the context of past climate changes. The Last Glacial Maximum (LGM) is known to have resulted in an enhancement of the dust deposition, especially over the polar regions. Using the Model for Interdisciplinary Research on Climate Earth System Model (MIROC-ESM), we investigated the impact of glaciogenic dust on the climate of the LGM and found that the effect of the enhancement of dust results in less cooling over the polar regions. One of the major reasons of the reduced cooling is the ageing of snow or ice, resulting in the reduction of the albedo by a high dust deposition, especially in the vicinity of high glaciogenic dust emissions. Although the net radiative perturbations in the lee of high glaciogenic dust provenances are negative, warming by ageing of snow overcomes this radiative perturbation in the Northern Hemisphere. In contrast, the radiative perturbation by the high dust loading in the troposphere acts to warm the surface surrounding Antarctica, which is mainly caused by the longwave aerosol–cloud interaction of dust and is likely the result of the greenhouse effect of the enhanced cloud fraction in the upper troposphere. Although our analysis mainly focused on the results of the experiments using the atmospheric part of the MIROC-ESM, we also conducted full MIROC-ESM experiments for a first trial of glacial dust modelling. The long-term trend to enhance warming in the Northern Hemisphere with the increase of glaciogenic dust was observed, whereas the warming level around Antarctica is almost unchanged, even after an extended interaction with the ocean.

1 Introduction

The Last Glacial Maximum (c.a. 21,000 years before present; LGM) is the distinct and most recent period featuring the maximum expansion of the land ice sheets in the Northern Hemisphere, and has been intensely investigated with the help of various paleo-proxy records and modelling studies (Braconnot et al., 2007a,b, Kageyama et al., 2006, 2017). Global warming is clearly an important driver for investigations seeking to clarify the mechanisms of climate change, as repeatedly stated in the assessment reports of the Intergovernmental Panel on Climate Change (IPCC) (IPCC, 2013). For this purpose, it is especially important to evaluate the ability of models to capture past climate sensitivity.

Both the collection of paleo-proxy data and modelling studies are required to properly understand past climates, with the focus here on modelling. General circulation models (GCM) are one of the most widely used tools for investigating the mechanisms of the climate and climate change. The development of increased computational resources enables us to develop models with a higher complexity, with various components of the climate able to be coupled interactively. Previous modelling works targeting the LGM tend to underestimate cooling especially over high latitudes compared with the proxy data (Masson-Delmotte et al., 2006, 2010). The importance of the dust and vegetation feedback is frequently pointed out in IPCC AR5 Chapter 5 (IPCC, 2013).

The effect of aerosols is one of the most uncertain factors on the radiative perturbation in estimates of global warming. Although mineral dust aerosol is not the most significant cause of warming, its effect is not negligible because it is the most abundant aerosol. For example, Mahowald et al. (2010) investigated the trend of the dust amount in the 20th century both from observations and modelling, and reported the increase of desert dust and a net negative radiative perturbation.

Ice and sediment core data suggest a clear enhancement of dust during the LGM, which is especially pronounced at high latitudes, reaching levels more than 20 times compared with the present day over Antarctica. The enhancement of deposition is less over lower latitudes, but still a few factors higher compared with the present day (Winckler et al., 2008), with the deposition flux greater towards higher latitudes (Lambert et al., 2008, Lamy et al., 2014, Dome Fuji Ice Core Project Members, 2017).

In earlier times, off-line aerosol models were used with the output of atmospheric general circulation models (AGCM) (Mahowald et al., 1999, Lunt and Valdes, 2002, Claquin et al., 2003) to simulate glacial dust aerosols. Although a higher dust amount was estimated during the LGM compared with the pre-industrial (PI) period, the dust amount over Antarctica was still underestimated. Claquin et al. (2003) used an off-line tracer transport model and estimated the radiative perturbation at the top of the atmosphere (TOA). Later, Mahowald et al. (2006a,b) used the Community Atmosphere Model (CAM3) coupled with a mixed-layer ocean model and an on-line aerosol module to estimate the glaciogenic dust flux (Mahowald et al., 2006a) and the aerosol–radiation interaction (Mahowald et al. 2006b). Their standard LGM experiment simulated underestimation of dust deposition flux especially over the high latitudes compared to a proxy data archive, DIRTMAP. Then, they postulated “glaciogenic dust” sources surrounding of ice sheets and glaciers, where supposed to generate substantial amount of moraine debris during glacial periods. They let emit various dust fluxes from different source area and obtained a best fit to the DIRTMAP deposition distribution. Although this estimate could conceal the other possible and non-introduced processes of dust source, it is still a big step forward to obtain reasonable representation of dust load in the atmosphere and deposition distribution. Takemura et al. (2009) used the Model for Interdisciplinary Research on Climate (MIROC) AGCM with the online aerosol module to determine the aerosol–radiation and aerosol–cloud interactions for the LGM and pre-industrial (PI) periods at the surface and tropopause for the first time, but underestimated the amount of dust over Antarctica. Yue et al. (2011) used an AGCM to estimate the aerosol–radiation interaction by dust, and reported a cooling effect. Hopcroft et al. (2015) investigated the aerosol–radiation interaction at the TOA using an AGCM and the land module of an earth system model (ESM), the Hadley Centre Global Environment Model, and suggested the necessity of analyses of aerosol–

Clim. Past Discuss., https://doi.org/10.5194/cp-2018-2
Manuscript under review for journal Clim. Past
Discussion started: 21 February 2018

cloud interaction as future work. We also note that previous works rarely discuss the total effect of dust on the climate. Lambert et al. (2013) pointed out the possibility of polar amplification by dust.

Previous studies have used an AGCM, an AGCM coupled with a slab ocean model, or an AGCM with the land module of an ESM. Consequently, the feedback of the aerosol to the ocean and sea ice and back to the atmosphere was not taken into account. Here, in addition to the AGCM experiments, we simulate the LGM with sensitivity experiments targeting the effect of dust using the full ESM for the first time. Moreover, we evaluate the effect of dust on the surface temperature in detail during the LGM for the first time.

The following section explains the model and experimental set-up. The resulting dust amount and deposition distribution are presented in Sect. 3.1, with the influence of the dust on the atmosphere described in Sect. 3.2, the radiative perturbation by dust described in Sect. 3.3, and the effect of glaciogenic dust on the ocean described in Sect. 3.4. The results of the simulations are summarised and discussed in Sect. 4.

2 Model and experimental design

2.1 Description of the MIROC-ESM

The MIROC-ESM (Watanabe et al., 2011) used here is the version submitted to the Coupled Model Intercomparison Project phase 5 (CMIP5), and the Paleoclimate Modelling Intercomparison Project phase 3 (PMIP3). The resolution of the atmosphere is T42 with 80 vertical levels, while that of the ocean is about 1° (256 x 192). While the model is capable of prognosing the carbon dioxide (CO_2) amount in the atmosphere, the atmospheric CO_2 is prescribed in our experimental set-up. The spatially explicit individual-based Dynamic Global Vegetation Model (SEIB-DGVM) is implemented into the system, and returns the leaf area index (LAI) back to the Minimal Advanced Treatments of Surface Interaction and Runoff (MATSIRO) land module. Also implemented is the on-line aerosol module Spectral Radiation-Transport Model for Aerosol Species (SPRINTARS) (Takemura et al., 2000, 2002, 2005, and 2009), which explicitly treats organic, black carbon and

Clim. Past Discuss., https://doi.org/10.5194/cp-2018-2
Manuscript under review for journal Clim. Past
Discussion started: 21 February 2018

mineral dust, sea-salt aerosols, sulfate and the precursor gases of sulfate. It is coupled with the radiation and cloud microphysical schemes to calculate the aerosol-radiation and aerosol-cloud interactions. In the calculation of the aerosol-radiation interaction, the refractive indices depending on wavelengths, size distributions, and hygroscopic growth are considered. Number concentrations for cloud droplets and ice crystals are prognostic variables as well as their mass mixing ratios, and changes in their radii and precipitation rates are calculated, i.e., aerosol-cloud interaction is taken into account. The processes correlated to the dust generation are the surface wind, the vegetation type, soil moisture, the LAI, and snow cover. Once dust is generated, it is transported by the atmospheric circulation, and deposits by the processes of wet and dry deposition, and gravitational settling.

In MATSIRO module, the effect of dirt in snow (ageing of snow) varies with the dirt concentration at the snow surface to fit to an observed relation between snow albedo and dirt concentration (Aoki et al., 2006). The dirt concentration in snow is calculated from the deposition fluxes of dust and soot calculated in SPRINTARS. The relative strength of the absorption coefficients for dust and soot (0.012 for dust and 0.988 for black carbon) are weighted to the deposition fluxes to obtain a radiatively effective amount of dirt in snow.

Oceanic biogeochemical process is not coupled with dust in the model. One needs an off-line model to evaluate the carbon uptake by dust.

2.2 Experimental design

We performed eight experiments, with five experiments using the AGCM part of the MIROC-ESM, and the other three using the full MIROC-ESM. The particular experiments labelled as PI.a and PI.e represent the 1850 A.D. control climate of the PI era, with PI.e having been submitted to CMIP5. The last 100-year climatology of sea-surface temperatures (SST) and the sea ice of the period submitted to CMIP5 are used as the boundary conditions for PI.a. The experiments labelled as LGM.e and LGM.a represent the LGM climate following the PMIP3 protocol (Abe-Ouchi et al., 2015). The LGM.e experiment has been submitted to CMIP5/PMIP3 (Sueyoshi et al., 2013). The LGM.a experiment is the AGCM experiment using the SST and sea ice taken from the PMIP3 LGM experiment (LGM.e). The LGM.e experiment has been extended for a further 800 years beyond the PMIP3 period (Fig. 1). The LGMglac.a experiment is a new experiment with the same conditions as LGM.a, but with an additional glaciogenic dust flux following Mahowald et al. (2006a). The LGMglac.naging.a and LGM.naging.a experiments have the same settings as LGMglac.a and LGM.a, but without the ageing effect of snow. The LGMglac.e experiment is the full ESM version of LGMglac.a, which branches from the LGM.e experiment 40 years prior to the period submitted to CMIP5/PMIP3 (Fig. 1). The glaciogenic dust flux from each area is set identical to the estimate of Mahowald et al. (2006a). The emission area is also consistent between the experiments, with little deviation following the land–sea mask of MIROC-ESM. There are three strong emission areas, the Pampas of South America, central North America and eastern Siberia. The integration of LGMglac.e was performed for 940 years. Table 1 lists the experiments.

3 Results

3.1 Dust amount and comparison with data archives

The emission flux of dust (g m-2 year-1) is shown in Figure 2 for the PI.a, LGM.a and LGMglac.a experiments. For the PI.a experiment, the major dust sources are the Saharan, Arabian, Gobi and Taklamakan Desert areas. A minor source is also found in the mid-latitude of South America. While these dust sources look reasonable based on the present-day situation, there is little dust emission from the plausible dust source of Australia. The wet bias over Australia in the PI.a experiment leads to excess vegetation, which prevents the emission of dust, and persists in the LGM.a and LGMglac.a experiments. In these experiments, the dust emission flux in the Saharan, Gobi and

Clim. Past Discuss., https://doi.org/10.5194/cp-2018-2
Manuscript under review for journal Clim. Past
Discussion started: 21 February 2018

Taklamakan Deserts is significantly enhanced, which is the result of a drier climate during the LGM, with an additional emission flux evident from northern Siberia. In contrast, the emission flux from South America is reduced, which is probably because of the increased soil moisture, resulting in an enhancement of precipitation enhancement in this region. For the LGMglac.a experiment, the glaciogenic dust emission is clearly evident surrounding the extended ice sheets during the LGM. The total emission amount is 80.6 (Mg s^{-1}) for the PI.a experiment, 230.0 (Mg s^{-1}) for the LGM.a experiment and 426.3 (Mg s^{-1}) for the LGMglac.a experiment. The change in the zonal mean dust loading in the atmosphere is shown in Figure 3 for the ratios LGM.a/PI.a (a), LGMglac.a/PI.a (b). In the LGM.a experiment, the dust mass concentration in the Northern Hemisphere is enhanced, but decreased in the Southern Hemisphere compared with the PI.a experiment. In contrast, the mass concentration enhanced significantly in both the northern and southern high latitudes in the LGMglac.a experiment. The higher uplift of the glaciogenic dust in the Southern Hemisphere compared with the Northern Hemisphere can be attributed to the different conditions of the strong dust sources, which, for the Southern Hemisphere, is exposed to the stronger wind speed resulting from the lack of continental land; in the Northern Hemisphere, the strong glaciogenic sources located over the continents are subject to lower wind speeds. The distribution of dust deposition for each experiment is shown in Figure 4 (a) (b) and (c), and the ratio to PI.a in Figure 5 in comparison with the archives of the ice and sediment core data as indicated by the coloured circles (Kohfeld et al., 2013, Albani et al., 2014). The scatter plots (Fig. 4 d, e, f) compare the data with the modelled deposition rate at the grids corresponding to the data locations. The colour and mark type are used for categorisation according to the area and the type of core data. A reasonable correlation is seen for the PI.a experiment, except in the grids over the Southern Ocean, which are mostly located in the southern Pacific Ocean region. The main location of the dust deposition in this region is expected to be Australia (Li et al., 2010, Albani et al., 2012), where our model underestimates the emission. In the LGM.a experiment, the dust deposition flux is underestimated in North America, Eurasia, the South Pacific, the Southern Ocean and Antarctica. In contrast, in

Clim. Past Discuss., https://doi.org/10.5194/cp-2018-2
Manuscript under review for journal Clim. Past
Discussion started: 21 February 2018

Climate of the Past Discussions

the LGMglac.a experiment, the underestimation is generally improved. The model-data linear correlation coefficients in the logarithmic scale are 0.79, 0.62 and 0.80 for the PI.a, LGM.a, and LGMglac.a experiments, respectively. The differences of the deposition flux between the PI.a and PI.e experiments, the LGM.a and LGM.e experiments, and the LGMglac.a and LGMglac.e experiments are almost negligible.

3.2 Effect of the increased amount of glacial dust on surface temperature

The surface temperature at a height of 2 m is influenced by the increased amount of glacial dust, with the difference of LGMglac.a relative to LGM.a presented in Fig. 6. The warming (i.e., less cooling compared with the PI.a results) is pronounced in the high latitudes in contrast to the expectation of the cooling effect of the dust. The changes in the LGMglac.a result relative to the LGM.a result for the net, longwave and shortwave downwards radiation at the surface are presented in Fig. 7. It represents the total effect of the glaciogenic dust on radiation towards the earth surface. Figure 7 showing a reduction in the shortwave radiation in the vicinity of the strong glaciogenic dust sources, as well as at the northern high latitudes and the edge of Antarctica. In contrast, the enhancement of the longwave radiation in the LGMglac.a experiment is pronounced surrounding Antarctica and in the northern high latitudes. While the reduced shortwave radiation dominates the net change in the vicinity of the glaciogenic emission area, the positive longwave change dominates the region surrounding Antarctica. The radiative perturbation by the dust is detailed in the next section.

Figure 8 shows that the warming of LGMglac.a−LGM.a south of 55° S is evident without the inclusion of the effects of the ageing of snow (LGMglac.naging.a−LGM.naging.a). This suggests that the warming around Antarctica is not the result of the ageing of snow. Figure 8 shows that the warming of LGMglac.a−LGM.a south of 55° S is evident without the inclusion of the effects of the ageing of snow (LGMglac.naging.a−LGM.naging.a). This suggests that the warming around Antarctica is not the result of the ageing of snow, but follows from the

Clim. Past Discuss., https://doi.org/10.5194/cp-2018-2
Manuscript under review for journal Clim. Past
Discussion started: 21 February 2018

change in the radiation balance in the atmosphere. Moreover, the magnitude of the warming is not significantly affected by ocean coupling (LGMglac.e−LGM.e).

In contrast, more than 80 % of the warming in the Northern Hemisphere is the result of the ageing of the snow surface as evident by inspection of the LGMglac.naging.a−LGM.naging.a results (Fig. 8). The high dust deposition rate reduces the albedo of the surface, and leads to the reduction of the shortwave reflected radiation, which overcomes the cooling effect of the dust loading in the atmosphere, resulting in warming. The warming in the Northern Hemisphere is the most pronounced over eastern Siberia and central North America, where a large amount of the glaciogenic dust is deposited, and therefore where the albedo of the LGMglac.a experiment is reduced significantly. The snow in the LGMglac.a experiment thaws earlier in the year than for the LGM.a experiment over eastern Siberia. A substantial amount of snow melted over a large area in this region, which accelerated the warming by the reduction in the albedo. In contrast, in central North America, the snow reduced compared with the LGM.a experiment, but is still significantly higher than the PI.a experiment. The position of the −2 °C isopleth averaged from June to August shifted northwards by about 1° latitude, which is significantly less than the model resolution. Here, we question whether the model is able to represent the appropriate ageing of snow under such a high dust deposition flux. As this is beyond the scope of our study, further evaluations of the effects of the ageing of snow are required.

3.3 Aerosol–radiation and aerosol–cloud interactions by dust

The aerosol–radiation and aerosol–cloud interactions are estimated using the same method as Takemura et al. (2009). The net global mean radiative perturbation (aerosol–radiation and aerosol–cloud) of dust is a cooling at the Earth's surface for all the experiments. The breakdown of the LGM experiments relative to the PI experiment for the change in the global mean radiative perturbation is listed in Table 2. The net change of the global mean aerosol–radiation interaction at the TOA is slightly positive for the LGM.a−PI.a results and amounts to 0.12 W

Clim. Past Discuss., https://doi.org/10.5194/cp-2018-2
Manuscript under review for journal Clim. Past
Discussion started: 21 February 2018

Climate of the Past Discussions

m^{-2} for the LGMglac.a−PI.a results. However, the changes at the surface are both negative (−0.21 W m^{-2} and −0.30 W m^{-2} with and without glaciogenic dust, respectively, which is close to the previous studies -0.25 and -0.56 W m^{-2} with and without glaciogenic dust in Mahowald et al. (2006b), -0.23 W m^{-2} (Takemura et al., 2009)), and are mainly caused by changes in the shortwave radiation. The net change of the global mean aerosol–cloud interaction at the TOA for the LGM.a−PI.a result is −0.36 W m^{-2}. Both the shortwave and longwave radiation increased with the glaciogenic dust, with the resulting net change of −0.39 W m^{-2}. At the surface, without glaciogenic dust, a net negative value reduced compared to the TOA. With the inclusion of glaciogenic dust, however, the change at the surface is a little more negative than the change at TOA. Considering the total effect of dust, but without glaciogenic dust, the radiative perturbation change at the TOA relative to the surface is small, whereas the inclusion of glaciogenic dust results in the cooling of the surface by the aerosol–radiation interaction. Figure 9 shows the spatial distribution of radiative perturbation by dust at the TOA, with a smaller difference between the LGMglac.a and LGM.a results compared with that at the surface (Figure 10 (a)). At the TOA, although the influence of glaciogenic dust from the Pampas region distributes over the Southern Ocean, the positive longwave and negative shortwave radiation almost cancel each other out. There are local negative effects at the strong glaciogenic dust sources, but the amplitudes are much smaller than at the surface (Fig. 10). Therefore, the action of the glaciogenic dust as seen at the surface occurs between the TOA and the Earth's surface. Therefore, we investigate the change in the spatial distribution and strength under different climatic conditions.

Except in the vicinity of massive dust sources, such as the Saharan Desert, the aerosol–cloud interaction dominates the radiative perturbation. Figure 10 shows the change of the net radiative perturbation at the surface for the LGMglac.a−LGM.a, LGMglac.a−PI.a and LGM.a−PI.a experiments. The additional glaciogenic dust worked to reduce the shortwave radiation. The negative radiative perturbation is distinct in the vicinity of the emission area. In contrast, for the longwave radiation, the general positive radiative perturbation resulting from the glaciogenic dust is obvious, especially in the vicinity of the strong dust sources, and at the edge of Antarctica. The negative shortwave radiation forcing overcomes the positive longwave radiation forcing in the vicinity of the glaciogenic sources. However, the positive longwave radiative perturbation plays a role in the regions surrounding Antarctica. The higher dust loading promotes the generation of cloud ice and high-level clouds, especially in the regions surrounding Antarctica, likely resulting in an enhanced greenhouse effect, which warms the lower troposphere (Fig. 3 (c), and Fig. 11).

3.4 Influence of glaciogenic dust on the ocean

We have extended the LGM.e experiment by 800 years beyond the original PMIP3 period (Fig. 1), and the LGMglac.e experiment by 940 years. The last 300 years averaged surface air temperature and SST changes according to the LGMglac.e–LGM.e results are presented in Fig. 12. Compared to a pollen proxy archive (Bartlein et al., 2011), the difference between LGM.e and LGMglac.e looks minor. Warming of the SST by the increased air temperature is obvious in the northern high latitudes, but the magnitude of the SST change is mostly below 0.5°C. A local strong warming along the Gulf Stream can be attributed to the difference of the thermohaline circulation strength. While we leave the investigation of the effect of dust on the thermohaline circulation for future work, we note that there may be a possibility of the effect of strong ageing of the snow in the Northern Hemisphere. In contrast, no change in the SST around Antarctica is calculated (Fig. 12 (f)), which confirms that the warming around Antarctica is not the result of the change in the temperature of the ocean. Even after the extended integration times of our simulations, the high plateau over the Antarctica, which is often the location of ice core sites, does not warm further (see circled alphabets in Fig. 12, a-c). The LGMglac.e cooling from the PI.e results for this area are more or less within the range of observational estimates (−7 to −10°C) (Stenni et al., 2010, Uemura et al., 2012).

The SSTs in the LGM.e and LGMglac.e experiments compared with the PI.e experiment both appear reasonable compared with the LGM SST reconstruction in coloured circles (MARGO project members, 2009) (Fig. 12 (d) (e)). A local cooling of the ocean temperature is seen in the lee of the glaciogenic dust source from Argentina, which would be caused by the negative radiative perturbation (Fig. 7 and 10 (a)).

4 Conclusion

We have used the MIROC-ESM to investigate the effect of mineral dust aerosol on the glacial climate. The representations of climatology by the PI.a and PI.e simulations are reasonable for a state-of-the-art ESM (Watanabe et al. 2011). The cooling evident in the LGM.e experiment compared with the PI.e results is also generally comparable with paleo-proxy archives (Fig. 12). We have mainly discussed the effect of the glaciogenic dust in the new experiments using the AGCM part of the MIROC-ESM in terms of the LGMglac.a results compared with the LGM.a results. The additional glaciogenic dust effect on the climate is mainly evident as a warming of the high latitudes in contrast to general expectations, and to that demonstrated by Mahowald et al. (2006b) as a zonal mean. Especially for the northern high latitudes, areas are warmed by the reduced albedo because of the snow surface covered by dust, and even the prolonged snow disappearance in certain seasons, which is especially pronounced in eastern Siberia. Although the longwave radiative perturbation worked negatively in the vicinity of the high glaciogenic dust flux sources, the ageing effect overcomes this cooling effect, resulting in a net increase in temperature.

The warming effect resulting from additional dust is also seen surrounding Antarctica, which is not attributable to the ageing of snow, but to the longwave aerosol–cloud interactions. Accounting for this effect would alter the distribution of the scatter evident in Figure 5.5(d) in the IPCC's Fifth Assessment Report, showing the importance of the eastern Antarctic cooling during the LGM for the climate.

Clim. Past Discuss., https://doi.org/10.5194/cp-2018-2
Manuscript under review for journal Clim. Past
Discussion started: 21 February 2018

Climate of the Past Discussions Open Access EGU

We have adopted additional dust sources from Mahowald et al. (2006a,b) as a first step, where their glaciogenic dust flux is identified to best fit to the data archives, but, as we have noted, it does not correspond well to the new proxy data at locations in the Southern Ocean. However, this mismatch may also be attributed to a feature of our model, i.e., insufficient dust emission from Australia, which is mainly caused by the overestimation of soil moisture and also by the resulting excess of plants. Our study draws attention to the high dust loading over the Southern Ocean affecting the increase in surface temperature surrounding the Antarctica, implying the need to investigate the climate sensitivity of the amount of dust emissions in future work. On the other hand over the Southern Ocean, the SST is hardly affected (Fig. 8) under the surface radiation change (Fig. 7 (a) and Fig. 10 (a)) probably because of the large heat capacity of ocean.

In the tropics, the dust effect on the surface temperature with an enhanced dust input is similar to what Mahowald et al. (2010) reported in studying the mid to late 20th century, but with a contrasting effect at high latitudes. The major difference is that the dust is enhanced at low latitudes, i.e., the Sahara-Sahel draught in the 20th century perturbation compared with the additional high dust inputs at high latitudes in our study, where the background albedo is high resulting from the extended snow and ice-covered areas.

In the MIROC-ESM, snow cover in the PI.e (PI.a) experiment tends to persist in the boreal spring over Siberia compared with a re-analyses data (Dee et al. 2011). This positive bias may influence the change we see in the LGM.e (LGM.a) and LGMglac.e (LGMglac.a) experiments.

The strong effect of the ageing of snow is especially significant in the Northern Hemisphere. Because snow ageing has been tuned to fit modern observations in Hokkaido, Japan (Aoki et al., 2003, 2006) in MIROC-ESM, a strong dust provenance in the vicinity of the snow-covered areas is lacking, such as the glaciogenic dust situation seen in the eastern Siberia. Therefore, the evaluation of the quantitative influence of ageing with various observational sites is needed.

Although we were unable to treat the effect of the iron supply to the ocean in this model, activating the iron-fertilization effect and enhancing the amount of plankton would influence CO_2 uptake especially over the Southern Ocean (Martin, 1990). The better representation of the distribution of dust deposition is possible as a boundary condition for off-line biogeochemical models to investigate CO_2 uptake, for example, in a more realistic version of the experiments by Oka et al. (2011). Further investigation of the non-negligible effect of the change in the size distribution of dust as pointed out in Hopcroft et al. (2015) may also be necessary.

Plant functional types are prognosed in the dynamic vegetation module but are not returned to the land module in the MIROC-ESM; i.e., the climate–vegetation interaction is limited. The importance of full vegetation coupling is pointed out in O'ishi and Abe-Ouchi (2013), suggesting the necessity of future models to evaluate the change of plant functional types and especially the effect on dust cycles.

Under global warming, the dust emission amount is uncertain (Woodward et al., 2005, Tegen et al., 2004, Jacobson and Streets, 2009, Liao et al., 2009, Mahowald et al., 2006a, Ito and Kok, 2017). Therefore, improving the understanding of dust processes in models of the past climate would be a way to reduce the uncertainty of projections into the future.

Acknowledgements:

This research is supported by the "Integrated Research Program for Advancing Climate Models (TOUGOU program)" from the Ministry of Education, Culture, Sports, Science and Technology (MEXT), Japan, and is also partly supported by the Japan Society for the Promotion of Science (JSPS) KAKENHI under Grant Number 17H06104. The model experiments are conducted on Earth Simulator of JAMSTEC. The authors are grateful for the help and inspiring discussions by the MIROC development team of JAMSTEC/U. Tokyo/NIES. We also thank R. Foreman, PhD, from Edanz Group (www.edanzediting.com/ac) for English reviewing of the manuscript.

References

Abe-Ouchi A., Saito F., Kageyama M., Braconnot P., Harrison S. P., Lambeck K., Otto-Bliesner B. L., Peltier W. R., Tarasov L., Peterschmitt J. Y. and Takahashi K. : Ice-sheet configuration in the CMIP5/PMIP3 Last Glacial Maximum experiments., Geoscientific Model Development, 8, 3621-3637, https://doi.org/10.5194/gmd-8-3621-2015, 2015.

Albani S., Mahowald N. M., Delmonte B., Maggi V. and Winckler G. : Comparing modeled and observed changes in mineral dust transport and deposition to Antarctica between the Last Glacial Maximum and current climates., Climate Dynamics, 38, 1731-1755, https://doi.org/10.1007/s00382-011-1139-5, 2012.

Albani S., Mahowald N. M., Perry A. T., Scanza R. A., Zender C. S., Heavens N. G., Maggi V., Kok J. F. and Otto-Bliesner B. L. : Improved dust representation in the Community Atmosphere Model., Journal of Advances in Modeling Earth Systems, 6, 541-570, https://doi.org/10.1002/2013ms000279, 2014.

Aoki T., Hachikubo A. and Hori M. : Effects of snow physical parameters on shortwave broadband albedos., Journal of Geophysical Research-Atmospheres, 108, https://doi.org/10.1029/2003jd003506, 2003.

Aoki T., Motoyoshi H., Kodama Y., Yasunari T. J., Sugiura K. and Kobayashi H. : Atmospheric Aerosol Deposition on Snow Surfaces and Its Effect on Albedo., Sola, 2, 13-16, https://doi.org/10.2151/sola.2006-004, 2006.

Bartlein P. J., Harrison S. P., Brewer S., Connor S., Davis B. A. S., Gajewski K., Guiot J., Harrison-Prentice T. I., Henderson A., Peyron O., Prentice I. C., Scholze M., Seppa H., Shuman B., Sugita S., Thompson R. S., Viau A. E., Williams J. and Wu H. : Pollen-based continental climate reconstructions at 6 and 21 ka: a global synthesis., Climate Dynamics, 37, 775-802, https://doi.org/10.1007/s00382-010-0904-1, 2011.

Braconnot P., Otto-Bliesner B., Harrison S., Joussaume S., Peterchmitt J. Y., Abe-Ouchi A., Crucifix M., Driesschaert E., Fichefet T., Hewitt C. D., Kageyama M., Kitoh A., Laine A., Loutre M. F., Marti O., Merkel U., Ramstein G., Valdes P., Weber S. L., Yu Y. and Zhao Y. : Results of PMIP2 coupled simulations of the Mid-Holocene and Last Glacial Maximum - Part 1: experiments and large-scale features., Climate of the Past, 3, 261-277, https://doi.org/10.5194/cp-3-261-2007, 2007a.

Braconnot P., Otto-Bliesner B., Harrison S., Joussaume S., Peterchmitt J. Y., Abe-Ouchi A., Crucifix M., Driesschaert E., Fichefet T., Hewitt C. D., Kageyama M., Kitoh A., Loutre M. F., Marti O., Merkel U., Ramstein G., Valdes P., Weber L., Yu Y. and Zhao Y. : Results of PMIP2 coupled simulations of the Mid-Holocene and Last Glacial Maximum - Part 2: feedbacks with emphasis on the location of the ITCZ and mid- and high latitudes heat budget., Climate of the Past, 3, 279-296, https://doi.org/10.5194/cp-3-279-2007, 2007b.

Bullard J. E. and Austin M. J. : Dust generation on a proglacial floodplain, West Greenland., Aeolian Research, 3, 43-54, https://doi.org/10.1016/j.aeolia.2011.01.002, 2011.

Claquin T., Roelandt C., Kohfeld K. E., Harrison S. P., Tegen I., Prentice I. C., Balkanski Y., Bergametti G., Hansson M., Mahowald N., Rodhe H. and Schulz M. : Radiative forcing of climate by ice-age atmospheric dust., Climate Dynamics, 20, 193-202, https://doi.org/10.1007/s00382-002-0269-1, 2003.

Dee D. P., Uppala S. M., Simmons A. J., Berrisford P., Poli P., Kobayashi S., Andrae U., Balmaseda M. A., Balsamo G., Bauer P., Bechtold P., Beljaars A. C. M., Van De Berg L., Bidlot J., Bormann N., Delsol C., Dragani R., Fuentes M., Geer A. J., Haimberger L., Healy S. B., Hersbach H., Holm E. V., Isaksen L., Kallberg P., Kohler M., Matricardi M., Mcnally A. P., Monge-Sanz B. M., Morcrette J. J., Park B. K., Peubey C., De Rosnay P., Tavolato C., Thepaut J. N. and Vitart F. : The ERA-Interim reanalysis: configuration and performance of the data assimilation system. Quarterly Journal of the Royal Meteorological Society 137, 553-597, https://doi.org/10.1002/qj.828, 2011.

Dome Fuji Ice Core Project members: Kawamura K., Abe-Ouchi A., Motoyama H., Ageta Y., Aoki S., Azuma N., Fujii Y., Fujita K., Fujita S., Fukui K., Furukawa T., Furusaki A., Goto-Azuma K., Greve R., Hirabayashi M., Hondoh T., Hori A., Horikawa S., Horiuchi K., Igarashi M., Iizuka Y., Kameda T., Kanda H., Kohno M., Kuramoto T., Matsushi Y., Miyahara M., Miyake T., Miyamoto A., Nagashima Y., Nakayama Y., Nakazawa T., Nakazawa F., Nishio F., Obinata I., Ohgaito R., Oka A., Okuno J., Okuyama J., Oyabu I., Parrenin F., Pattyn F., Saito F., Saito T., Sakurai T., Sasa K., Seddik H., Shibata Y., Shinbori K., Suzuki K., Suzuki T., Takahashi A., Takahashi K., Takahashi S., Takata M., Tanaka Y., Uemura R., Watanabe G., Watanabe O., Yamasaki T., Yokoyama K., Yoshimori M., Yoshimoto T. and Dome Fuji Ice Core P. : State dependence of climatic instability over the past 720,000 years from Antarctic ice cores and climate modeling. Science Advances 3, https://doi.org/10.1126/sciadv.1600446, 2017.

Hopcroft P. O., Valdes P. J., Woodward S. and Joshi M. M. : Last glacial maximum radiative forcing from mineral dust aerosols in an Earth system model. Journal of Geophysical Research-Atmospheres 120, 8186-8205, https://doi.org/10.1002/2015jd023742, 2015.

IPCC, 2013: Climate Change 2013: The Physical Science Basis. Contribution of Working Group I to the Fifth Assessment Report of the Intergovernmental Panel on Climate Change [Stocker, T.F., D. Qin, G.-K. Plattner, M. Tignor, S.K. Allen, J. Boschung, A. Nauels, Y. Xia, V. Bex and P.M. Midgley (eds.)]. Cambridge University Press, Cambridge, United Kingdom and New York, NY, USA, 1535 pp, https://doi.org/10.1017/CBO9781107415324, 2013.

Ito A. and Kok J. F.: Do dust emissions from sparsely vegetated regions dominate atmospheric iron supply to the Southern Ocean? Journal of Geophysical Research-Atmospheres 122, 3987-4002, https://doi.org/10.1002/2016JD025939, 2017.

Kageyama M., Albani S., Braconnot P., Harrison S. P., Hopcroft P. O., Ivanovic R. F., Lambert F., Marti O., Peltier W. R., Peterschmitt J. Y., Roche D. M., Tarasov L., Zhang X., Brady E. C., Haywood A. M., Legrande A. N., Lunt D. J., Mahowald N. M., Mikolajewicz U., Nisancioglu K. H., Otto-Bliesner B. L., Renssen H., Tomas R. A., Zhang Q., Abe-Ouchi A., Bartlein P. J., Cao J., Li Q., Lohmann G., Ohgaito R., Shi X. X., Volodin E., Yoshida K. and Zheng W. P. : The PMIP4 contribution to CMIP6-Part 4: Scientific objectives and experimental design of the PMIP4-CMIP6 Last Glacial Maximum experiments and PMIP4 sensitivity experiments. Geoscientific Model Development 10, 4035-4055, https://doi.org/10.5194/gmd-10-4035-2017, 2017.

Jacobson, M. Z., and Streets, D. G.: Influence of future anthropogenic emissions on climate, natural emissions, and air quality. Journal of Geophysical Research-Atmospheres, 114, https://doi.org/10.1029/2008JD011476, 2009.

Kageyama M., Laine A., Abe-Ouchi A., Braconnot P., Cortijo E., Crucifix M., De Vernal A., Guiot J., Hewitt C. D., Kitoh A., Kucera M., Marti O., Ohgaito R., Otto-Bliesner B., Peltier W. R., Rosell-Mele A., Vettoretti G., Weber S. L., Yu Y. and

Members M. P. : Last Glacial Maximum temperatures over the North Atlantic, Europe and western Siberia: a comparison between PMIP models, MARGO sea-surface temperatures and pollen-based reconstructions. Quaternary Science Reviews 25, 2082-2102, https://doi.org/10.1016/j.quascirev.2006.02.010, 2006.

Kohfeld K. E., Graham R. M., De Boer A. M., Sime L. C., Wolff E. W., Le Quere C. and Bopp L. : Southern Hemisphere westerly wind changes during the Last Glacial Maximum: paleo-data synthesis. Quaternary Science Reviews 68, 76-95, https://doi.org/10.1016/j.quascirev.2013.01.017, 2013.

Lambert F., Delmonte B., Petit J. R., Bigler M., Kaufmann P. R., Hutterli M. A., Stocker T. F., Ruth U., Steffensen J. P. and Maggi V. : Dust-climate couplings over the past 800,000 years from the EPICA Dome C ice core. Nature 452, 616-619, https://doi.org/10.1038/nature06763, 2008.

Lambert F., Kug J. S., Park R. J., Mahowald N., Winckler G., Abe-Ouchi A., O'ishi R., Takemura T. and Lee J. H.: The role of mineral-dust aerosols in polar temperature amplification. Nature Climate Change 3, 487-491, https://doi.org/10.1038/nclimate1785, 2013.

Lamy F., Gersonde R., Winckler G., Esper O., Jaeschke A., Kuhn G., Ullermann J., Martinez-Garcia A., Lambert F. and Kilian R. : Increased Dust Deposition in the Pacific Southern Ocean During Glacial Periods. Science 343, 403-407, https://doi.org/10.1126/science.1245424, 2014.

Li F. Y., Ramaswamy V., Ginoux P., Broccoli A. J., Delworth T. and Zeng F. R.: Toward understanding the dust deposition in Antarctica during the Last Glacial Maximum: Sensitivity studies on plausible causes. Journal of Geophysical Research-Atmospheres 115, https://doi.org/10.1029/2010JD014791, 2010.

Liao H., Zhang Y., Chen W. T., Raes F. and Seinfeld J. H.: Effect of chemistry-aerosol-climate coupling on predictions of future climate and future levels of tropospheric ozone and aerosols. Journal of Geophysical Research-Atmospheres 114, 10.1029/2008JD010984 2009.

Lunt D. J. and Valdes P. J.: Dust deposition and provenance at the Last Glacial Maximum and present day. Geophysical Research Letters 29, https://doi.org/10.1029/2002gl015656, 2002.

Mahowald N., Kohfeld K., Hansson M., Balkanski Y., Harrison S. P., Prentice I. C., Schulz M. and Rodhe H. : Dust sources and deposition during the last glacial maximum and current climate: A comparison of model results with paleodata from ice cores and marine sediments. Journal of Geophysical Research-Atmospheres 104, 15895-15916, https://doi.org/10.1029/1999jd900084, 1999.

Mahowald N. M., Muhs D. R., Levis S., Rasch P. J., Yoshioka M., Zender C. S. and Luo C. : Change in atmospheric mineral aerosols in response to climate: Last glacial period, preindustrial, modern, and doubled carbon dioxide climates. Journal of Geophysical Research-Atmospheres 111, https://doi.org/10.1029/2005jd006653, 2006a.

Mahowald N. M., Yoshioka M., Collins W. D., Conley A. J., Fillmore D. W. and Coleman D. B. : Climate response and radiative forcing from mineral aerosols during the last glacial maximum, pre-industrial, current and doubled-carbon dioxide climates. Geophysical Research Letters 33, https://doi.org/10.1029/2006gl026126, 2006b.

Mahowald N. M., Kloster S., Engelstaedter S., Moore J. K., Mukhopadhyay S., Mcconnell J. R., Albani S., Doney S. C., Bhattacharya A., Curran M. A. J., Flanner M. G., Hoffman F. M., Lawrence D. M., Lindsay K., Mayewski P. A., Neff J., Rothenberg D., Thomas E., Thornton P. E. and Zender C. S. : Observed 20th century desert dust variability: impact on climate and biogeochemistry. Atmospheric Chemistry and Physics 10, 10875-10893, https://doi.org/10.5194/acp-10-10875-2010, 2010.

MARGO project members: Waelbroeck C., Paul A., Kucera M., Rosell-Mele A., Weinelt M., Schneider R., Mix A. C., Abelmann A., Armand L., Bard E., Barker S., Barrows T. T., Benway H., Cacho I., Chen M. T., Cortijo E., Crosta X., De Vernal A., Dokken T., Duprat J., Elderfield H., Eynaud F., Gersonde R., Hayes A., Henry M., Hillaire-Marcel C., Huang C. C., Jansen E., Juggins S., Kallel N., Kiefer T., Kienast M., Labeyrie L., Leclaire H., Londeix L., Mangin S., Matthiessen J., Marret F., Meland M., Morey A. E., Mulitza S., Pflaumann U., Pisias N. G., Radi T., Rochon A., Rohling E. J., Sbaffi L., Schaefer-Neth C., Solignac S., Spero H., Tachikawa K., Turon J. L. and Members M. P. : Constraints on the magnitude and patterns of ocean cooling at the Last Glacial Maximum. Nature Geoscience 2, 127-132, https://doi.org/10.1038/ngeo411, 2009.

Martin, J. H.: Glacial-Interglacial CO2 change: The iron hypothesis. Paleoceanography, 5(1), 1-13, https://doi.org/10.1029/PA005i001p00001, 1990.

Masson-Delmotte V., Kageyama M., Braconnot P., Charbit S., Krinner G., Ritz C., Guilyardi E., Jouzel J., Abe-Ouchi A., Crucifix M., Gladstone R. M., Hewitt C. D., Kitoh A., Legrande A. N., Marti O., Merkel U., Motoi T., Ohgaito R., Otto-Bliesner B., Peltier W. R., Ross I., Valdes P. J., Vettoretti G., Weber S. L., Wolk F. and Yu Y. : Past and future polar amplification of climate change: climate model intercomparisons and ice-core constraints. Climate Dynamics 26, 513-529, https://doi.org/10.1007/s00382-005-0081-9, 2006.

Masson-Delmotte V., Stenni B., Pol K., Braconnot P., Cattani O., Falourd S., Kageyama M., Jouzel J., Landais A., Minster B., Barnola J. M., Chappellaz J., Krinner G., Johnsen S., Rothlisberger R., Hansen J., Mikolajewicz U. and Otto-Bliesner B.: EPICA Dome C record of glacial and interglacial intensities. Quaternary Science Reviews 29, 113-128, https://doi.org/10.1016/j.quascirev.2009.09.030, 2010.

O'Ishi, R., & Abe-Ouchi, A.: Influence of dynamic vegetation on climate change and terrestrial carbon storage in the Last Glacial Maximum. Climate of the Past, 9(4), 1571-1587, https://doi.org/10.5194/cp-9-1571-2013. 2013.

Oka A., Abe-Ouchi A., Chikamoto M. O. and Ide T. : Mechanisms controlling export production at the LGM: Effects of changes in oceanic physical fields and atmospheric dust deposition. Global Biogeochemical Cycles 25, https://doi.org/10.1029/2009gb003628, 2011.

Stenni B., Masson-Delmotte V., Selmo E., Oerter H., Meyer H., Rothlisberger R., Jouzel J., Cattani O., Falourd S., Fischer H., Hoffmann G., Iacumin P., Johnsen S. J., Minster B. and Udisti R. : The deuterium excess records of EPICA Dome C and Dronning Maud Land ice cores (East Antarctica). Quaternary Science Reviews 29, 146-159, https://doi.org/ 10.1016/j.quascirev.2009.10.009, 2010.

Sueyoshi T., Ohgaito R., Yamamoto A., Chikamoto M. O., Hajima T., Okajima H., Yoshimori M., Abe M., O'ishi R., Saito F., Watanabe S., Kawamiya M. and Abe-Ouchi A. : Set-up of the PMIP3 paleoclimate experiments conducted using an Earth system model, MIROC-ESM. Geoscientific Model Development 6, 819-836, https://doi.org/10.5194/gmd-6-819-2013, 2013.

Takemura T., Egashira M., Matsuzawa K., Ichijo H., O'ishi R. and Abe-Ouchi A.: A simulation of the global distribution and radiative forcing of soil dust aerosols at the Last Glacial Maximum. Atmospheric Chemistry and Physics 9, 3061-3073, https://doi.org/10.5194/acp-9-3061-2009, 2009.

Takemura T., Nakajima T., Dubovik O., Holben B. N. and Kinne S.: Single-scattering albedo and radiative forcing of various aerosol species with a global three-dimensional model. Journal of Climate 15, 333-352, https://doi.org/10.1175/1520-0442(2002)015<0333:ssaarf>2.0.co;2, 2002.

Takemura T., Nozawa T., Emori S., Nakajima T. Y. and Nakajima T. : Simulation of climate response to aerosol direct and indirect effects with aerosol transport-radiation model. Journal of Geophysical Research-Atmospheres 110, https://doi.org/10.1029/2004JD005029, 2005.

Takemura T., Okamoto H., Maruyama Y., Numaguti A., Higurashi A. and Nakajima T.: Global three-dimensional simulation of aerosol optical thickness distribution of various origins. Journal of Geophysical Research-Atmospheres 105, 17853-17873, https://doi.org/10.1029/2000jd900265, 2000.

Tegen I., Werner M., Harrison S. P. and Kohfeld K. E. : Relative importance of climate and land use in determining present and future global soil dust emission. Geophysical Research Letters 31, 2004.

Uemura R., Masson-Delmotte V., Jouzel J., Landais A., Motoyama H. and Stenni B.: Ranges of moisture-source temperature estimated from Antarctic ice cores stable isotope records over glacial-interglacial cycles. Climate of the Past 8, 1109-1125, https://doi.org/10.5194/cp-8-1109-2012, 2012.

Watanabe S., Hajima T., Sudo K., Nagashima T., Takemura T., Okajima H., Nozawa T., Kawase H., Abe M., Yokohata T., Ise T., Sato H., Kato E., Takata K., Emori S. and Kawamiya M. : MIROC-ESM 2010: model description and basic results of CMIP5-20c3m experiments. Geoscientific Model Development 4, 845-872, https://doi.org/10.5194/gmd-4-845-2011, 2011.

Werner M., Tegen I., Harrison S. P., Kohfeld K. E., Prentice I. C., Balkanski Y., Rodhe H. and Roelandt C. : Seasonal and interannual variability of the mineral dust cycle under present and glacial climate conditions. Journal of Geophysical Research-Atmospheres 107, https://doi.org/10.1029/2002jd002365, 2002.

Winckler G., Anderson R. F., Fleisher M. Q., Mcgee D. and Mahowald N. : Covariant glacial-interglacial dust fluxes in the equatorial Pacific and Antarctica. Science 320, 93-96, https://doi.org/10.1126/science.1150595, 2008.

Woodward S., Roberts D. L. and Betts R. A.: A simulation of the effect of climate change-induced desertification on mineral dust aerosol. Geophysical Research Letters 32, https://doi.org/10.1029/2005GL023482 2005.

Yue X., Wang H. J., Liao H. and Jiang D. B. : Simulation of the Direct Radiative Effect of Mineral Dust Aerosol on the Climate at the Last Glacial Maximum. Journal of Climate 24, 843-858, https://doi.org/10.1175/2010jcli3827.1, 2011.

Clim. Past Discuss., https://doi.org/10.5194/cp-2018-2
Manuscript under review for journal Clim. Past
Discussion started: 21 February 2018

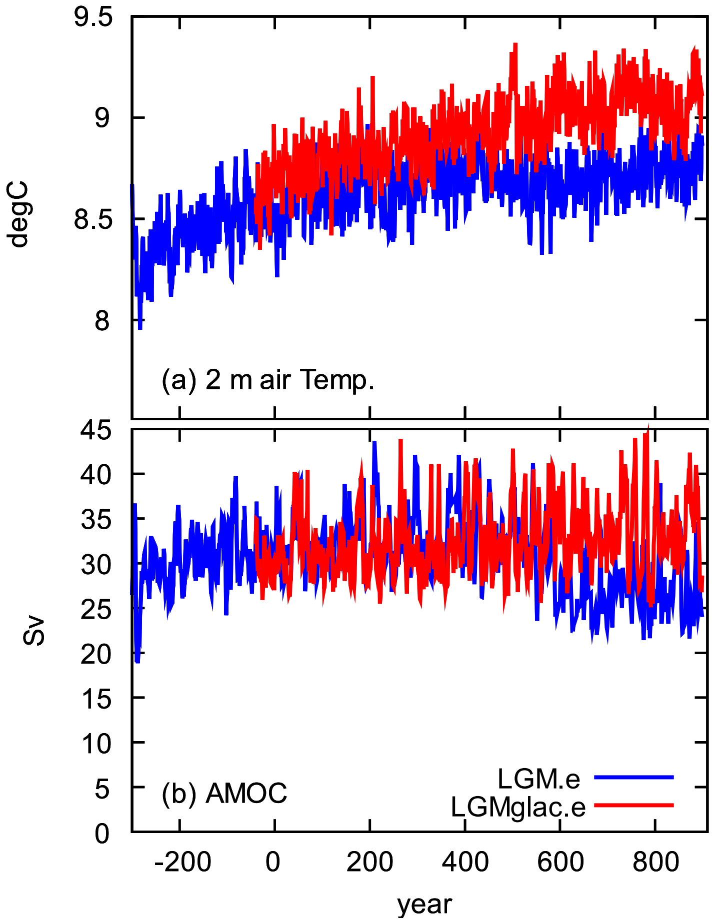

Figure 1: The time series of (a) global mean annual mean temperature at 2 m height (degree C) and of (b) the peak strength of the Atlantic meridional overturning circulation (Sv), for LGM.e and LGMglac.e. The year zero is set to the beginning of the period submitted to CMIP5.

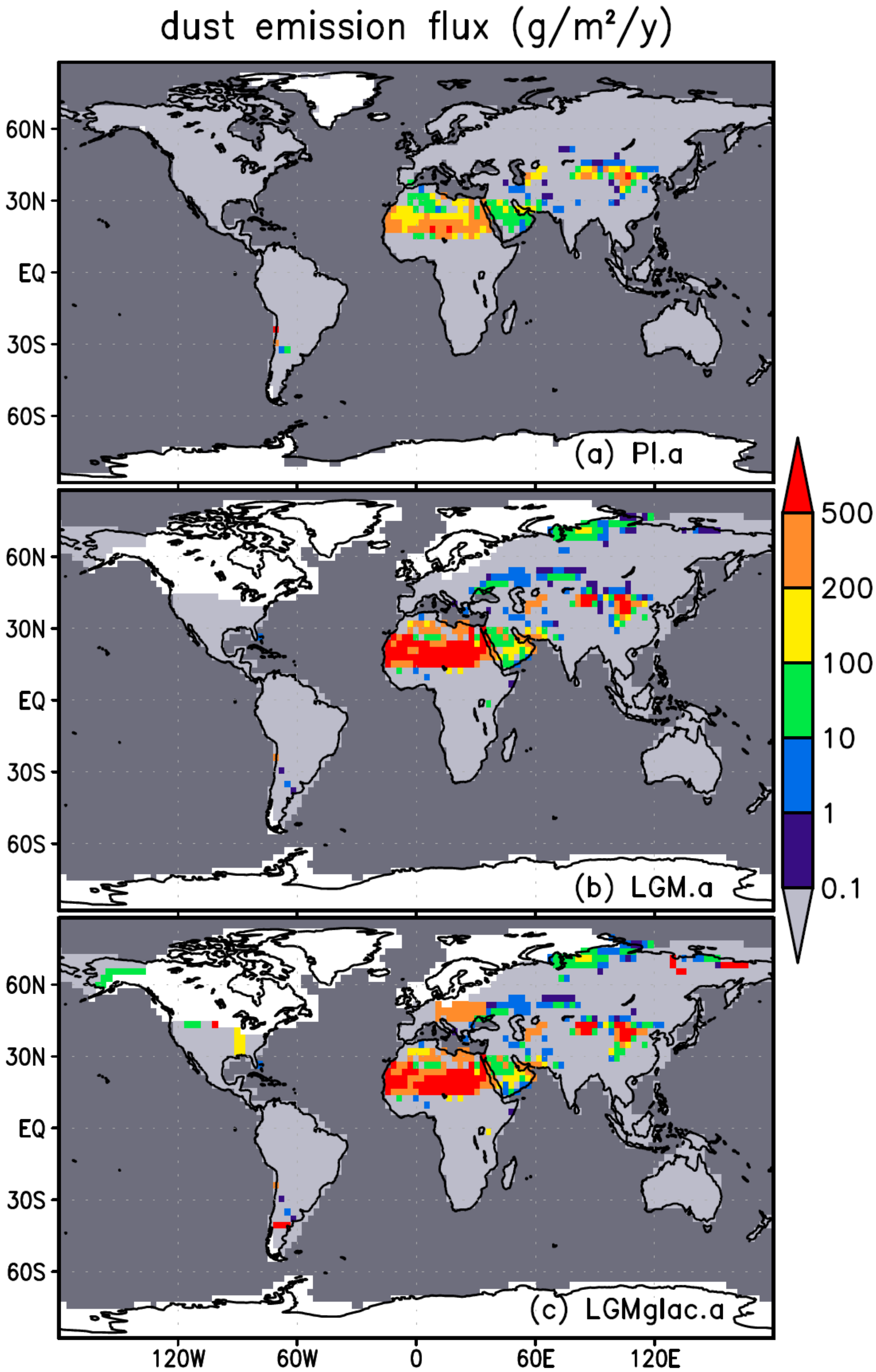

Figure 2: The dust emission flux (g m-2 year-1) for (a) PI.a, (b) LGM.a and (c) LGMglac.a. The oceanic area is coloured with dark gray. The ice sheet area is coloured with white.

Clim. Past Discuss., https://doi.org/10.5194/cp-2018-2
Manuscript under review for journal Clim. Past
Discussion started: 21 February 2018

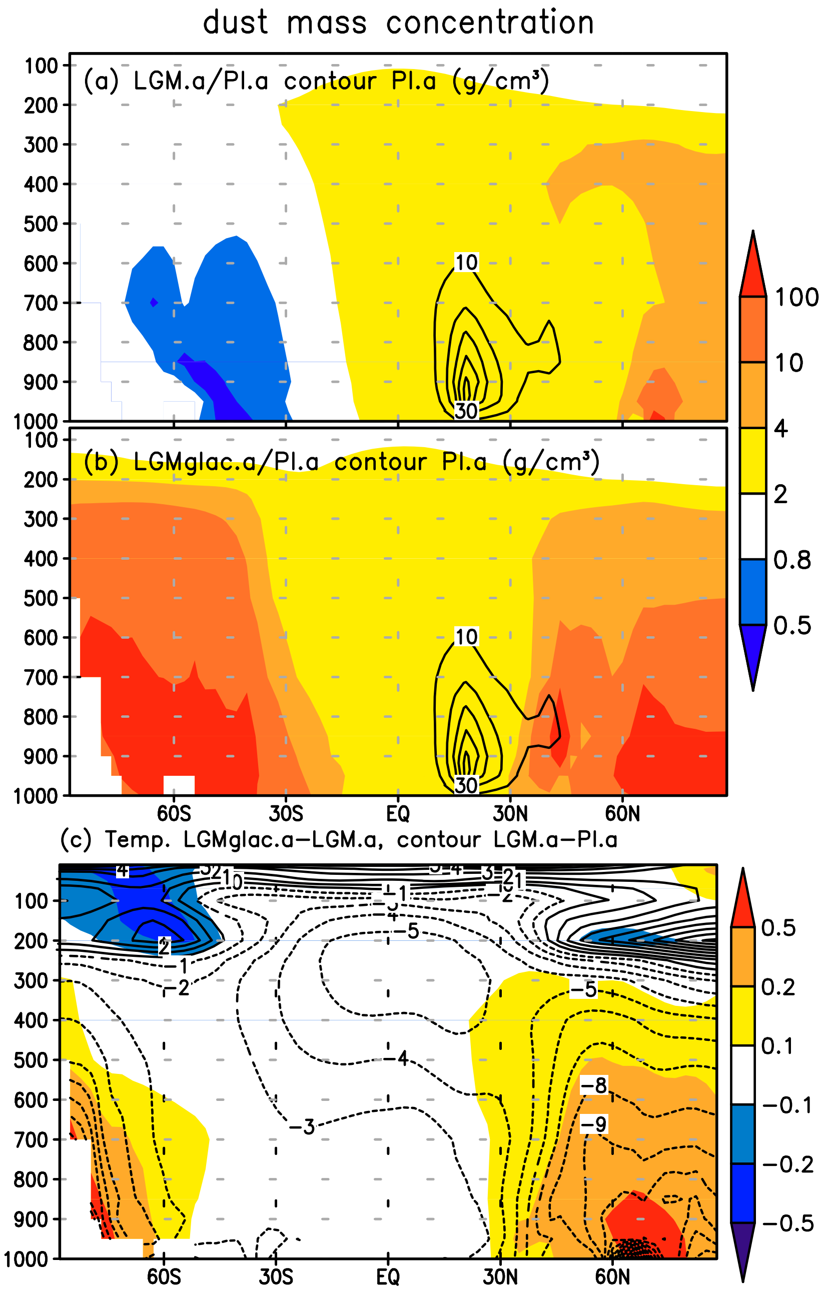

Figure 3: All panels are zonal mean-height plots. Ratio of the dust mass concentration for (a) LGM.a/PI.a, (b) LGMglac.a/PI.a and (c) temperature change for LGMglac.a-LGM.a. The contour lines in (a) and (b) is the dust mass concentration for PI.a (g cm-3) and in (c) is the temperature change for LGM.a-PI.a (oC).

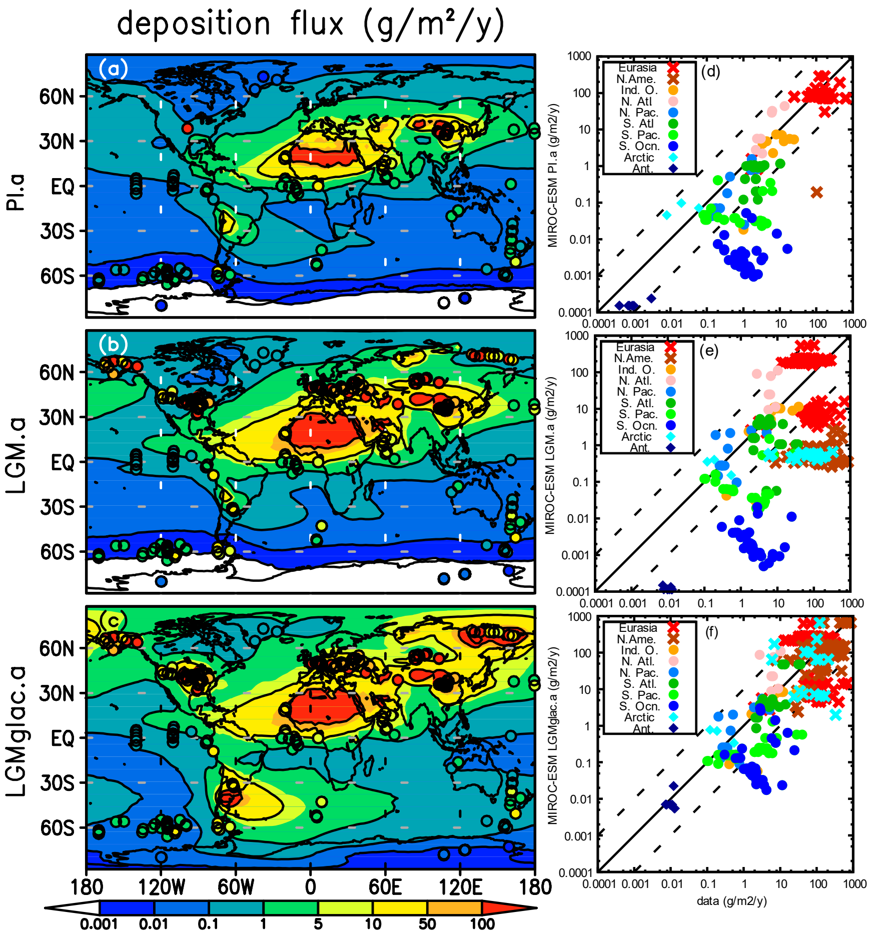

Figure 4: The model-data comparison of the dust deposition flux (g m^{-2} year^{-1}) estimated from the ice and sediment core data archives obtained from Kohfeld et al. 2013 and Albani et al. 2014. The map for the (a) PI.a (b) LGM.a(c)

Clim. Past Discuss., https://doi.org/10.5194/cp-2018-2
Manuscript under review for journal Clim. Past
Discussion started: 21 February 2018

LGMglac.a. The data-model scatter plots for (d) PI.a(e) LGM.a and (f) LGMglac.a. The colours and marks represent area and core types. Red for Eurasia, brown for North America, orange for the Indian Ocean, pink and light blue for the Atlantic and the Pacific Oceans in the northern hemisphere, Green and light green for the Atlantic and the Pacific Oceans in the southern hemisphere, blue for the Southern Ocean and turquoise blue for the Arctic and dark blue for the Antarctica. Crosses represents terrestrial sediment core, circles for the marine sediment core and diamonds for the ice core data.

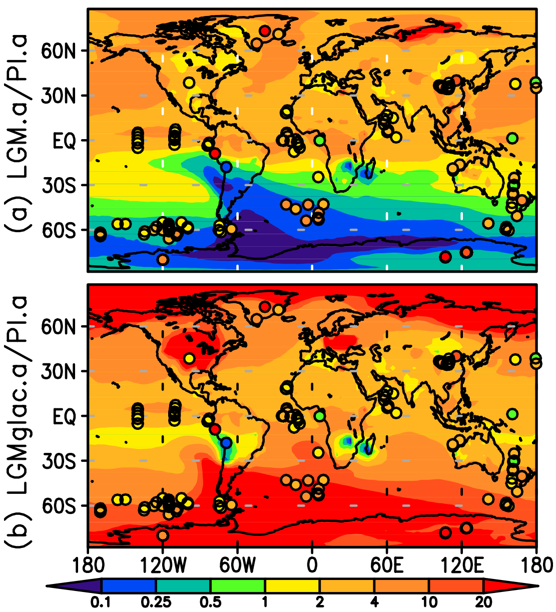

Figure 5: The model-data comparison of ratio of the dust deposition flux estimated from the ice and sediment core data archives obtained from Kohfeld et al. (2013) and Albani et al. (2014). The map for ratio (a) LGM.a/PI.a. (b) LGMglac.a/PI.a.

Clim. Past Discuss., https://doi.org/10.5194/cp-2018-2
Manuscript under review for journal Clim. Past
Discussion started: 21 February 2018

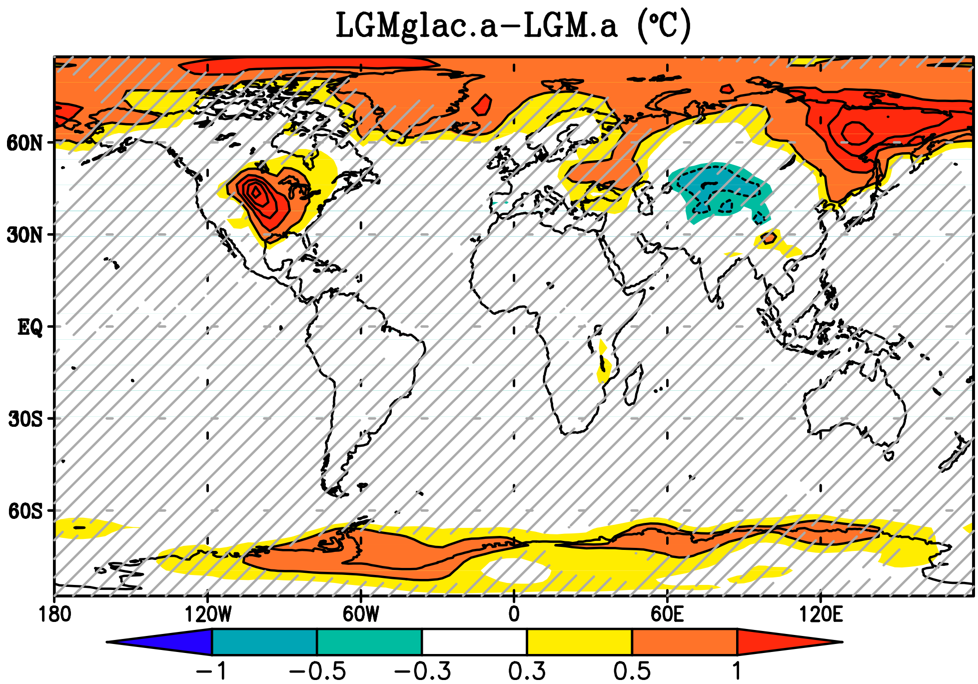

Figure 6: The difference of the surface temperature at 2 m height for LGMglac.a-LGM.a. The change is not significant at the hatched area by t-test in 95 % confidence.

Clim. Past Discuss., https://doi.org/10.5194/cp-2018-2
Manuscript under review for journal Clim. Past
Discussion started: 21 February 2018

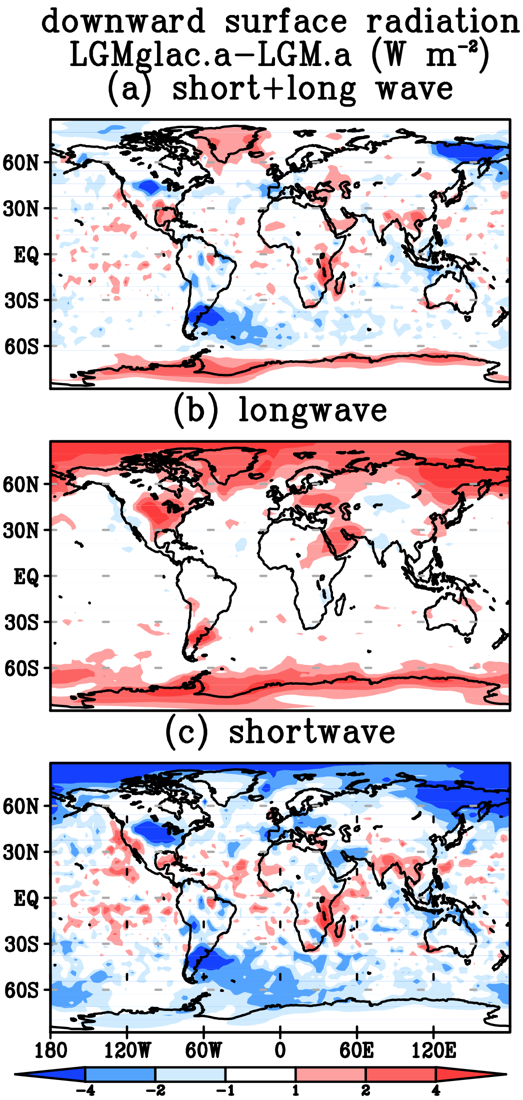

Figure 7: the change in the (a) net, (b) longwave and (c) shortwave downward radiation at the surface LGMglac.a-LGM.a (W m-2) (downward, positive).

Clim. Past Discuss., https://doi.org/10.5194/cp-2018-2
Manuscript under review for journal Clim. Past
Discussion started: 21 February 2018

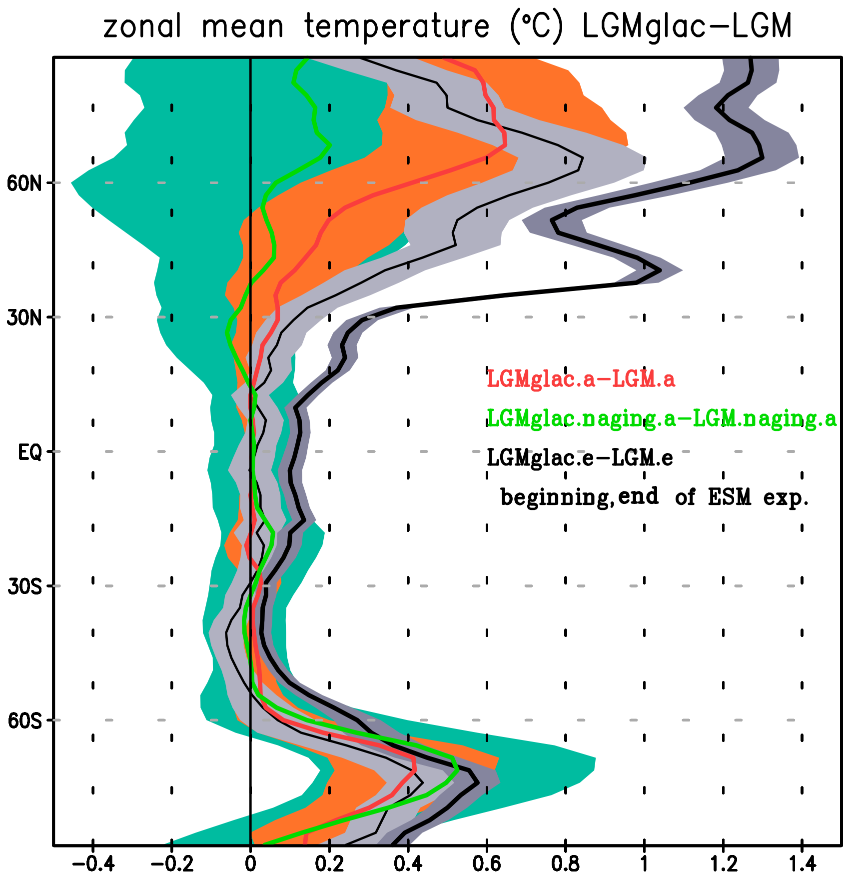

Figure 8: 2 m air temperature difference between LGMglac and LGM. Red line denotes LGMglac.a-LGM.a. Green line denotes LGMglac.naging.a-LGM.naging.a, which means the change arose from non-aging effect of snow albedo. Thin and thick black lines denote LGMglac.e-LGM.e at the beginning (1 to 100th year average in Figure 1) and the end (701 to 900th year average) of the experiments, respectively. Shades represent the year to year standard deviation.

.

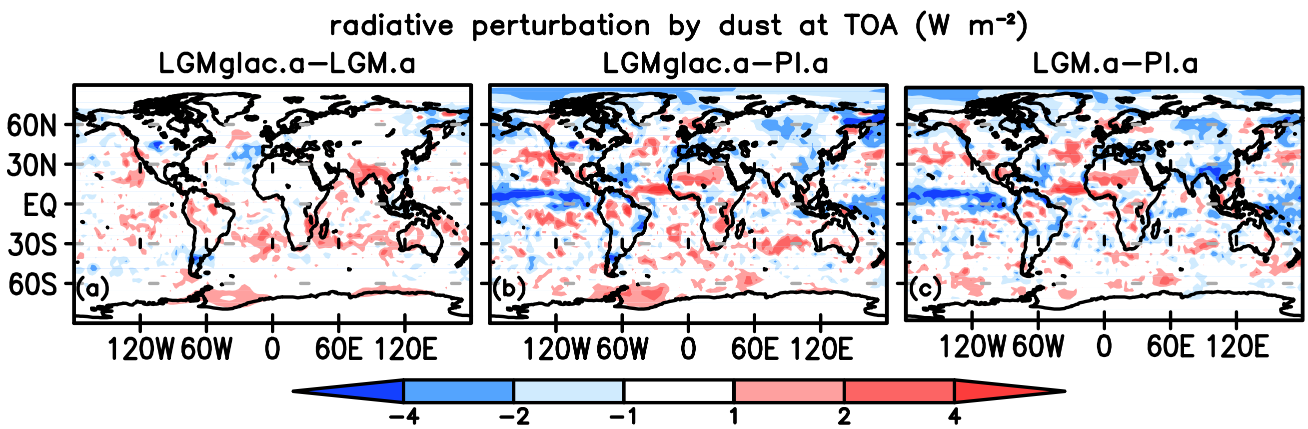

Fig. 9: Change of the net radiative perturbation by dust at the top of the atmosphere for (a) LGMglac.a-LGM.a (b) LGMglac.a-PI.a and (c) LGM.a-PI.a.

Clim. Past Discuss., https://doi.org/10.5194/cp-2018-2
Manuscript under review for journal Clim. Past
Discussion started: 21 February 2018

Climate of the Past Discussions
Open Access

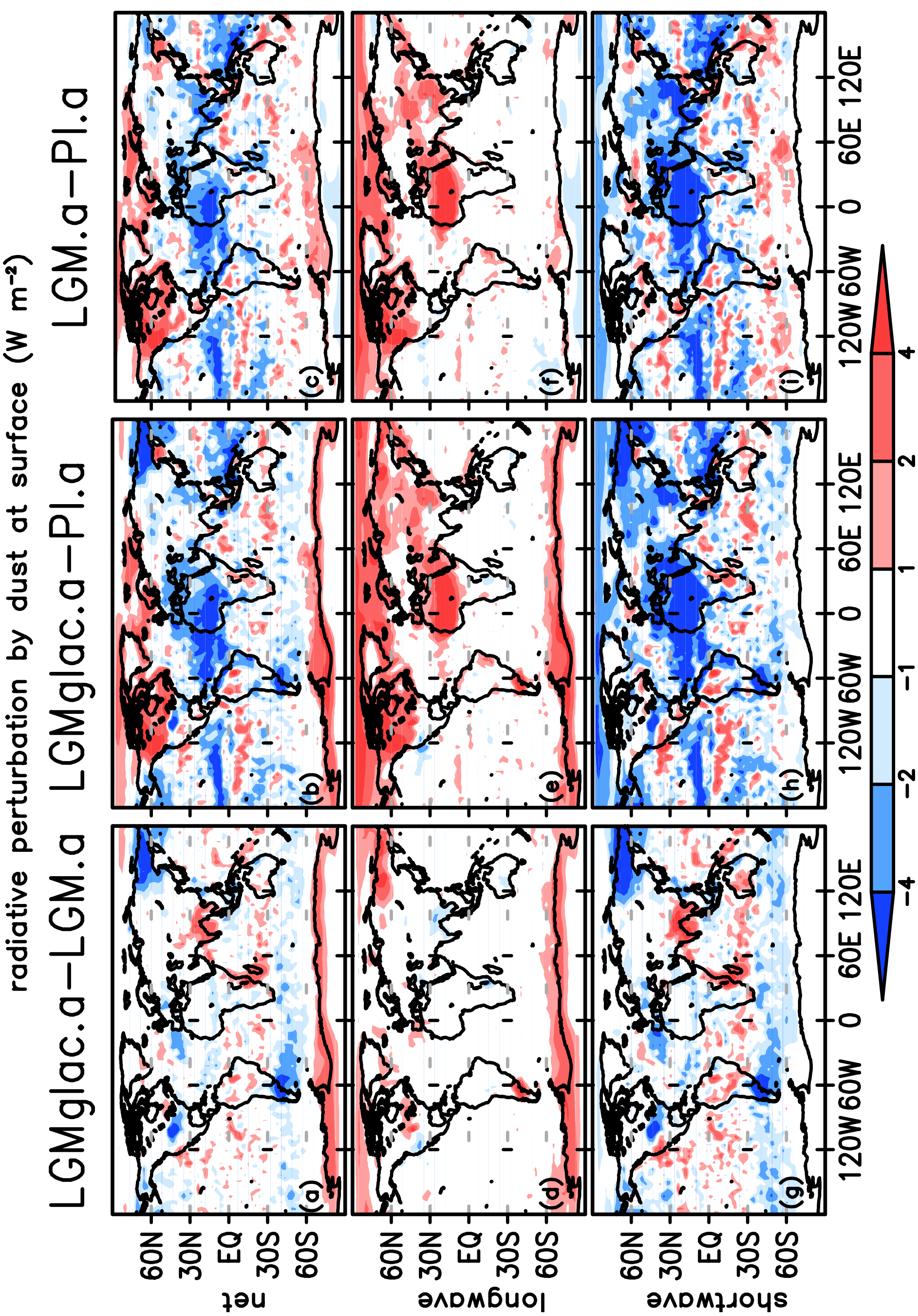

Figure 10: Change of the net radiative perturbation by dust at the surface for (a) LGMglac.a-LGM.a (b) LGMglac.a-PI.a and (c) LGM.a-PI.a. The decomposition of the net change for the longwave for (d) LGMglac.a-LGM.a (e) LGMglac.a-PI.a and (f) LGM.a-PI.aand for the shortwave for (g) LGMglac.a-LGM.a (h) LGMglac.a-PI.a (i) LGM.a-PI.a.

Clim. Past Discuss., https://doi.org/10.5194/cp-2018-2
Manuscript under review for journal Clim. Past
Discussion started: 21 February 2018

Climate of the Past Discussions
Open Access
EGU

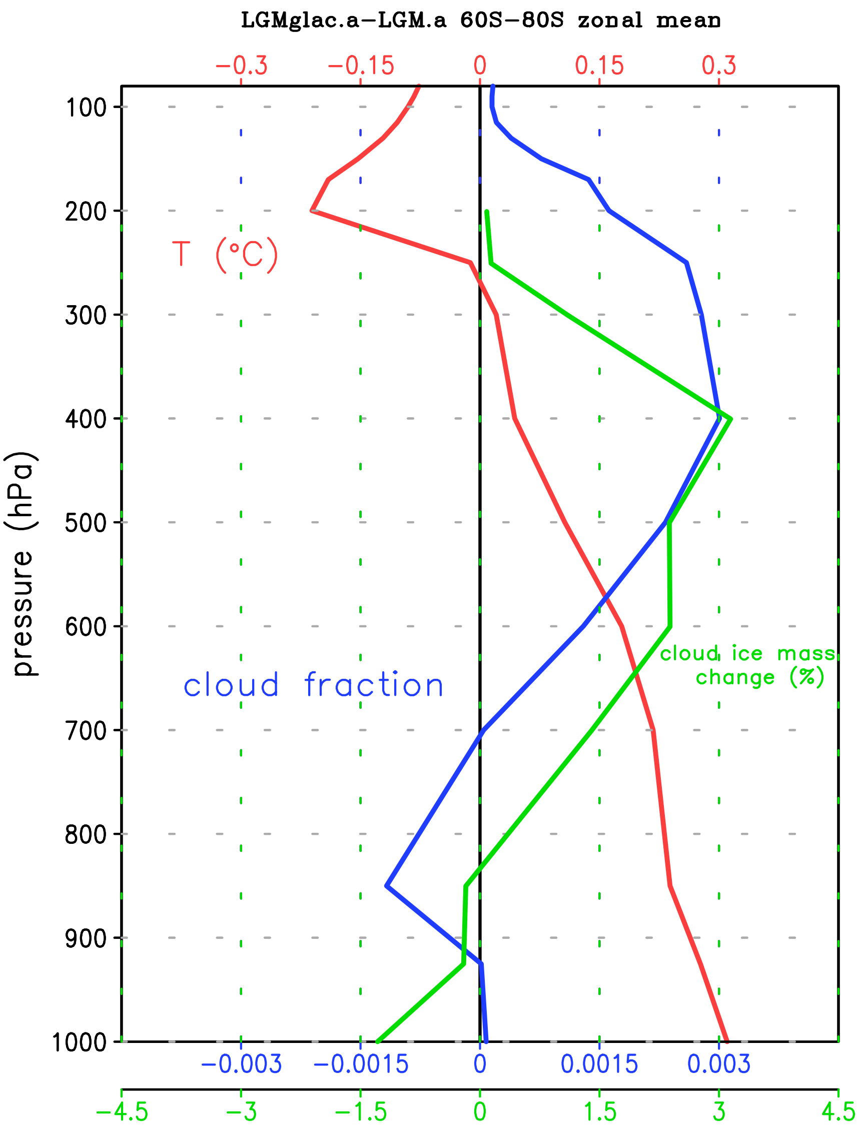

Figure 11: 60° S-80° S averaged value-height plot for change in LGMglac.a-LGM.a for the temperature in red, cloud fraction in blue and cloud ice mass concentration in green. Note that the cloud ice mass concentration is plotted only at the value exceed 1e-8 kg kg^{-1} in LGM.a.

5 .

Clim. Past Discuss., https://doi.org/10.5194/cp-2018-2
Manuscript under review for journal Clim. Past
Discussion started: 21 February 2018

Climate of the Past
Discussions
Open Access

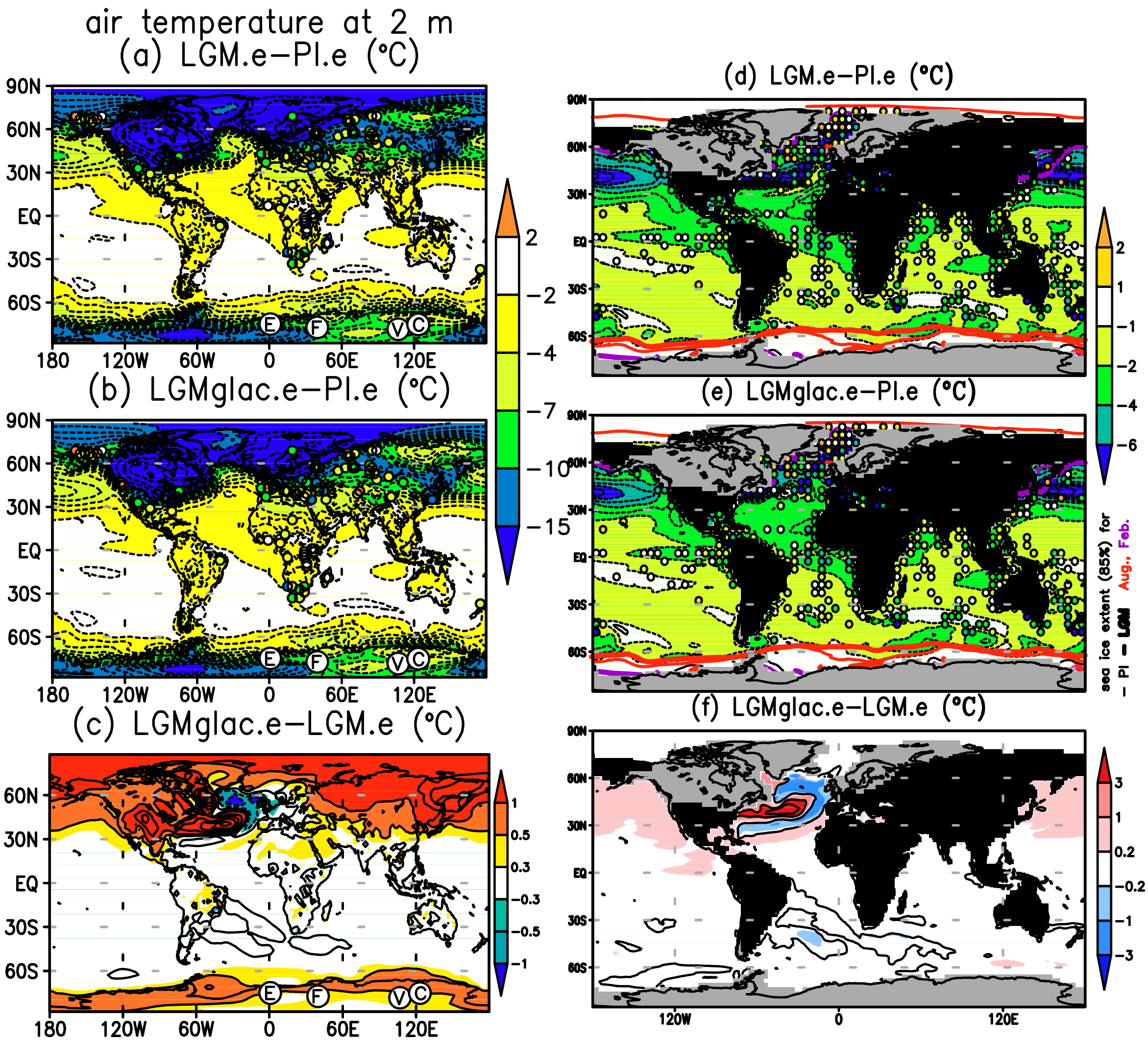

Figure 12: The difference of the surface temperature at 2 m height for (a) LGM.e-PI.e (b) LGMglac.e-PI.e and (c) LGMglac.e-LGM.e. Colored circles represent reconstructed temperature change by pollen proxy archives (Bartlein et al., 2011). Circled alphabets on the Antarctica represents four ice core locations. E for EDML, F for Dome Fuji, V for Vostok, and C for Dome C. The sea surface temperature changes for (d) LGM.e-PI.e, (e) LGMglac.e-PI.e and (f) LGMglac.e-LGM.e. The purple and red lines in (d) and (e) are 85 % sea ice concentration in February and August for PI (thin) and LGM (thick), respectively. Colored circles represent MARGO SST reconstruction (MARGO project members, 2009). Gray area represents ice sheet covered area.

Clim. Past Discuss., https://doi.org/10.5194/cp-2018-2
Manuscript under review for journal Clim. Past
Discussion started: 21 February 2018

Table 1: list of experiments

(a) Experiment using MIROC-ESM

Experiment names	**Explanation**	**Integration length (years)**
PI.e	The piControl experiment submitted to CMIP5	530
LGM.e	The lgm experiment submitted to CMIP5/PMIP3. The integration is extended further 800 years	1200
LGMglac.e	LGM.e + adding glaciogenic dust flux following Mahowald et al. (2006a)	940

(b) Experiments using AGCM part of MIROC-ESM

Experiment names	**Explanation**
PI.a	Pre-industrial control, SST, sea ice and LAI are taken from the climatology of
LGM.a	The lgm experiment submitted to CMIP5/PMIP3. The integration is extended further 800 years
LGMglac.a	LGM.e + adding glaciogenic dust flux following Mahowald et al. (2006a)
LGM.naging.a	LGM.a + no ageing of snow albedo
LGMglac.naging.a	LGMglac.a + no ageing of snow albedo

Table 2: LGMglac.a-PI.a and LGM.a-PI.a changes in global mean radiative perturbation by dust at the (a) surface and (b) the top of atmosphere (W m^{-2}).

(a) surface	**LGMglac.a-PI.a Aerosol-radiation**	**LGM.a-PI.a Aerosol-radiation**	**LGMglac.a-PI.a Aerosol-cloud**	**LGM.a-PI.a Aerosol-cloud**
net	-0.30	-0.21	-0.42	-0.28
Long wave	0.37	0.28	0.50	0.34
Short wave	-0.67	-0.50	-0.92	-0.62

(b) TOA	**LGMglac.a-PI.a Aerosol-radiation**	**LGM.a-PI.a Aerosol-radiation**	**LGMglac.a-PI.a Aerosol-cloud**	**LGM.a-PI.a Aerosol-cloud**
net	0.12	0.07	-0.39	-0.36
Long wave	0.17	0.14	0.62	0.26
Short wave	-0.05	-0.07	-1.01	-0.63